values of pd. At any rate, Kachickas in his thesis gives a sparking potential of 35.0 kv for $pd=960$ cm mm Hg for "moderate ultraviolet illumination." Considering that Kachickas used a different cathode than we did, this agreement seems very consistent with our measurements of F^*, G^*, and γ^*.

Thus although a detailed study has not been made, the indications are that the Townsend breakdown condition satisfactorily describes the breakdown mechanism in electron-attaching gases.

One may now see why oxygen has a breakdown potential as low as that of air or nitrogen. While attachment reduces primary ionization currents, γ is so high in oxygen as to compensate for the effect of attachment.

PHYSICAL REVIEW VOLUME 111, NUMBER 2 JULY 15, 1958

Model for the Surface Potential Barrier and the Periodic Deviations in the Schottky Effect*

P. H. CUTLER† AND J. J. GIBBONS
Department of Physics, The Pennsylvania State University, University Park, Pennsylvania

(Received March 17, 1958)

Although most of the features of the observed periodic deviations in the Schottky effect are in good agreement with predicted behavior, there is still disagreement between theory and experiment in the phase and amplitude of the deviations. It has been suggested that a possible origin of this difficulty is the use of the simple image force barrier at the surface of the metal. In this paper a model for the surface potential barrier is developed which is based on the quantum-mechanical calculation made by Bardeen on the form of the potential at the surface of a sodium-like metal, and the analysis of Sachs and Dexter on the quantum limits of the image-force theory. Employing this model, the periodic deviations are recalculated using essentially the mathematical formalism developed by Juenker and his co-workers. Certain computational refinements are introduced in the averaging of the transmission coefficient. The results are compared with previous theory and experiment in terms of two parameters which characterize the form of the surface potential; the surface reflection coefficient $|\mu|$ which appears as a factor in the amplitude, and the phase factor δ. These computed values are 0.6 and 2.6 respectively, as compared to single mean experimental values of 0.4 and 2.2 for the highly refractory metals, and to previous theoretical values of 0.2 and 3.7. The surface reflection coefficient calculated for the present model is in satisfactory agreement with recent experiments on the elastic scattering of slow electrons from the surface of a metal.

I. INTRODUCTION

THE increase in saturation thermionic emission from a metal with applied field strength was explained by Schottky as due to the lowering of the potential barrier at the surface by the external electric field. When careful measurements are taken on the variation of the current density, j, with the applied field, F, the plot of $\log j$ against $F^{\frac{1}{2}}$ is not a straight line as predicted by the simple Schottky theory, but instead one finds small oscillations about a straight line which increase in amplitude and period as F is increased. Guth and Mullin,[1] using the free electron model of a metal and a one-dimensional classical image potential, accounted for the periodic deviations as due to the interference between electron waves reflected from the barrier maximum and those reflected from a region of steep potential gradient near the surface of the metal.

The analysis of the experimental data on the Schottky deviations was made physically clearer when the theory was reformulated in terms of a total transmission coefficient defined by Herring and Nichols.[2] They expressed the transmission coefficient in terms of two complex reflection coefficients, one of which, λ, depends upon the potential in the region of barrier maximum, and μ, which depends upon the form of the potential near the emitter surface. Stated in this way, the effect of each reflecting region upon such experimentally measurable quantities as the period, phase, and amplitude of the deviations can be clearly identified.

The theory has been modified in terms of the revised transmission coefficient by Juenker, Colladay, and Coomes,[3] Juenker,[4] and Miller and Good.[5] Their results gave the correct period of the deviations and also agreed with the observed variation of the amplitude with field and temperature.[3,4,6,7] However, quantitatively the observed amplitudes and phase of the deviations did not agree with the theory. A possible source of the disagreement might have been the validity of the WKB approximation used in both the original Guth-

* This paper is based on a dissertation submitted by P. H. Cutler in partial fulfillment of the requirements for the degree of Doctor of Philosophy in the Department of Physics of The Pennsylvania State University.

† Haloid Fellow in Solid State Physics.

[1] E. Guth and C. J. Mullin, Phys. Rev. **59**, 575 (1941).

[2] C. Herring and M. H. Nichols, Revs. Modern Phys. **21**, 185 (1949).

[3] Juenker, Colladay, and Coomes, Phys. Rev. **90**, 772 (1953). This reference will hereafter be referred to as JI.

[4] D. W. Juenker, Phys. Rev. **99**, 1155 (1955). This reference will hereafter be referred to as JII.

[5] S. C. Miller and R. H. Good, Phys. Rev. **92**, 1367 (1953).

[6] Munick, La Berge, and Coomes, Phys. Rev. **80**, 887 (1950).

[7] Brock, Houde, and Coomes, Phys. Rev. **89**, 851 (1953).

Mullin[1] theory and in JI and JII. Miller and Good,[5] however, making use of the more exact WKB-type approximations[8] in recalculating the periodic deviations, obtained essentially the same results as in JI and JII. Since they used the same potential model as Juenker *et al.*, the agreement removes any uncertainty about the mathematical approximations.

It has been suggested[7] that a possible origin of the disagreement lies in the use of the simple image-force potential in the immediate neighborhood of the surface. Herring[2,9] has discussed the general behavior of an effective one-dimensional potential which an electron encounters moving through the surface of a metal. The qualitative features of this model are based upon general quantum-mechanical considerations and the results of Bardeen's[10] Hartree-Fock calculation of the charge density in the double layer at the surface of a monovalent metal.

More recently, Sachs and Dexter[11] have calculated an approximate quantum-mechanical correction to the classical image-force interaction energy which varies inversely with the square of the electron's distance from the surface. Using a correction term of this form, and imposing conditions of continuity with the internal potential of the metal, we obtain a potential function which has qualitative agreement with the Bardeen one-dimensional form. Furthermore, the coefficient of the correction term chosen in our work is shown to have the same sign and order of magnitude as the coefficient computed by the methods of Sachs and Dexter. It is here pertinent to observe that the actual three-dimensional problem has been reduced to an effective one-dimensional model which can only be justified by the success of its predictions over a fair range of experiments.

In the present paper the periodic deviations of the thermionic Schottky effect are recalculated using the new model for the potential barrier and some of the mathematical formalism developed by Juenker, Colladay, and Coomes in JI and JII. However, the surface reflection coefficient μ is here obtained by means of an exact solution of the Schrödinger equation for the potential region near the surface where the field term can be neglected. In addition certain modifications of the energy-averaging process employed in JI and JII are introduced. The mathematical forms of the deviation terms are essentially unchanged but the new potential model yields better agreement with experimental results in the phase and amplitudes of the deviations.

The proposed model for the surface potential barrier is discussed in Sec. II. In Sec. III the details for the calculation of μ are given. The parameter λ and the correction to the phase factor δ, defined in JI and JII, are derived in Sec. IV. The energy-averaging of the transmission coefficient is performed in Sec. V and the deviation terms are derived in Sec. VI. A discussion of the results is given in Sec. VII.

II. MODEL FOR THE SURFACE POTENTIAL BARRIER

When an electron is at large distances from the surface of a metal, the dominant long-range force exerted on it is due to the induced mirror-image charge on the metal, but within a distance of a few angstroms from the surface the short-range potential fields which the electron encounters can no longer be represented by the classical image force. Several theoretical attempts[12] have been made to determine the charge distribution at the surface of a metal, from which one could then obtain the form of the short-range potential field. Two methods which have been used most frequently are the Fermi-Thomas statistical model of a metal and the more refined wave-mechanical treatment. Bardeen[10] has made the most rigorous quantum treatment and the qualitative features of his results have general application. By including exchange-correlation effects Bardeen finds a one-dimensional effective potential asymptotic to the image potential at large distances outside the surface and approaching a constant value inside the metal. The electronic charge density which he calculates has a maximum just beneath the surface resulting in a corresponding shallow minimum in the potential function. Thus the effective potential obtained by Bardeen has the correct asymptotic form and the properties that (1) it keeps the force on the electron finite near the surface, and (2) it exhibits a potential minimum in the surface region. The solid curve in Fig. 1 describes the Bardeen-type potential.

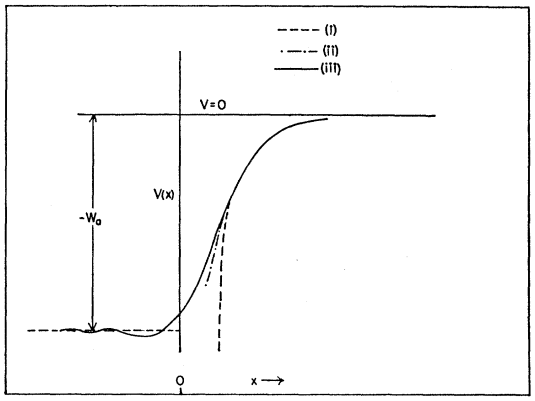

FIG. 1. Behavior of the electronic potential energy function in the neighborhood of a metal surface according to: (i) simple classical image-force theory, (ii) the image-force with the Sachs-Dexter correction term, and (iii) the Bardeen-Herring effective potential.

[8] S. C. Miller and R. H. Good, Phys. Rev. **91**, 174 (1953).
[9] C. Herring, in *Metal Interfaces* (American Society for Metals, Cleveland, 1952), pp. 1–19.
[10] J. Bardeen, Phys. Rev. **49**, 653 (1936).
[11] R. G. Sachs and D. L. Dexter, J. Appl. Phys. **21**, 1304 (1950).
[12] See reference 2, Chap. IV, p. 228.

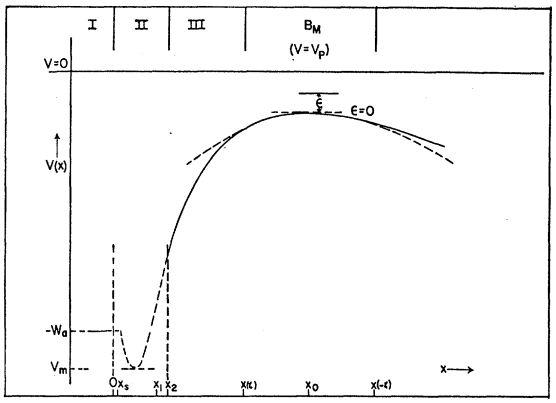

FIG. 2. Proposed model for the potential energy barrier of an electron near the surface of a metal (not drawn to scale). An electron escaping from the metal with total energy $W=V(x_0)+\epsilon$ passes through the constant potential region I and into the surface reflection region II. Beyond II, the electron moves in the predominantly mirror-image nonreflecting potential of region III, and then into the region of the barrier maximum, B_M, where electrons having small energy, ϵ, can suffer reflection. As in JI and JII, the potential in B_M is approximated by the parabolic potential V_p, shown by the dashed curve. The potential in II is joined to $-W_a$ and V_p at x_s and x_2 (here, as in JII, x_2 is taken equal to x_1).

Sachs and Dexter have treated the problem of the quantum limits of the electrostatic image force theory. They obtain a correction term $\Delta_1 E$ which gives the order-of-magnitude deviation from the classical image formula due to purely quantum-mechanical effects in the metal. This first-order correction to the interaction energy is of the form $\kappa^{\frac{1}{2}}x^{-1}|W(x)|$, where x is the distance of the electron from the surface, $W(x)$ is the classical image force energy, and $\kappa^{\frac{1}{2}}$ is a parameter depending on the properties of the metal. When $\kappa^{\frac{1}{2}}$ is positive, the resulting potential energy function exhibits the correct behavior as it approaches the surface, i.e., the force on the electron becomes less than the classical image force. The form of the Sachs-Dexter potential is given by the dashed curve in Fig. 1. Although Sachs and Dexter formally set up an equation which in theory would allow one to compute the potential function continuously through the surface and into the metal, the final expression they obtain is only applicable outside the surface because of the approximations which must be used in the derivation.

These considerations have led to the following choice for the effective potential energy function in the region outside the metal:

$$V(x)=-e^2(4x)^{-1}+\eta e^2(4x^2)^{-1}-eFx, \tag{1}$$

where $-e$ is the value of the electronic charge and F is the electric field strength. The parameter η in the correction term would be expected to depend upon the surface properties of the metal. $V(x)$ must be made to join the constant electrostatic potential energy $-W_a$ inside the metal.

Near the surface the contribution to the potential due to the field term can be neglected. The continuity of $V(x)$ and $-W_a$ then gives the equation for finding the join point:

$$x_s=\tfrac{1}{2}x_1\{1\pm[1-4\eta(x_1)^{-1}]^{\frac{1}{2}}\}, \tag{2}$$

where x_1 is $e^2(4W_a)^{-1}$. Note that x_1 as defined here would have been the join point of the classical image potential and $-W_a$. The resulting model for the potential is shown in Fig. 2.

It is realized that the addition of a simple η/x^2 term will not yield the correct potential in the immediate neighborhood of the surface. However, when the negative sign is chosen in (2) there are introduced the two relevant features of the Bardeen analysis, the finite force on the electron and a potential minimum in the surface region.

If we restrict η to positive real values, then from Eq. (1) we have

$$0\leq\eta\leq\tfrac{1}{4}x_1. \tag{3}$$

Values of $\eta\simeq 0$ introduce a physically implausible potential and in the limit $V(x)$ reduces to the usual image-force model. By choosing $\eta\lesssim\frac{1}{4}x_1$, the Sachs-Dexter type correction term yields a total potential in general qualitative agreement with the Bardeen potential.

Moreover, the larger value of η is indicated on a physical basis by the computation Sachs and Dexter make for $\Delta_1 E$. Their result for a point-charge interaction is

$$\Delta_1 E=\text{const}\kappa^{\frac{1}{2}}x^{-1}|W(x)|, \tag{4}$$

where $\kappa^{\frac{1}{2}}$ is evaluated by applying a Fermi-Thomas statistical model to the metal electrons. The values of $[\text{const}\kappa^{\frac{1}{2}}]$, which should correspond to η, are computed in the Sachs-Dexter approximation to be $\simeq 0.41\times10^{-8}$ cm for the three metals tungsten, tantalum, and molybdenum. However, values as high as this render impossible the joining of the external potential to W_a. The highest allowed values we can choose for η and join the potentials are $\eta\lesssim\frac{1}{4}x_1$. This makes $\eta\simeq 0.09\times10^{-8}$ cm for W, Ta, and Mo.

There is an additional argument which tends to justify the larger value of the parameter η. The depth of the potential well is related to η by the equation

$$V_m=-x_1(4\eta)^{-1}W_a, \tag{5}$$

where V_m is the value of $V(x)$ at the potential minimum. From the calculations of Bardeen[10] or of Juretschke[13] one can find the approximate value of V_m for a monovalent metal like sodium. For V_m they obtain about 1.1 W_a, and the corresponding value of η would be $\simeq\frac{1}{4}x_1$. Even if the well depth is varied from 1.1 W_a to 1.3 W_a, the value of η is very nearly the same. These small variations in η do not significantly change any final results in the computations in this paper.

[13] H. J. Juretschke, Phys. Rev. **92**, 1140 (1953).

III. DISCUSSION OF THE PARAMETER μ

A. Derivation of μ

The calculation of μ proceeds from the following assignment for the potential in the vicinity of the surface (see Fig. 2). The zero of $V(x)$, when $F=0$, is taken at $x=\infty$.

I. The potential to the left of the join point x_s is a constant:

$$V=-W_a \quad \text{for} \quad x\leq x_s. \tag{6}$$

II. The potential in the region of the minimum is considered to be independent of applied field:

$$V(x)\cong -e^2(4x)^{-1}+\eta e^2(4x^2)^{-1} \quad \text{for} \quad x_s\leq x\leq x_2 \tag{7}$$

where x_2 denotes the beginning of a region in which the probability of electron reflection is small.

III. To the right of x_2 the potential is

$$V(x)=-e^2(4x)^{-1}+\eta e^2(4x^2)^{-1}-eFx \quad \text{for} \quad x_2\leq x. \tag{8}$$

In region I we take the plane wave solutions of the Schrödinger equation to be

$$\psi_{\mathrm{I}}=e^{i\kappa x}+\mu e^{-i\kappa x}, \tag{9}$$

with time factor $e^{-i\omega t}$. Since the total energy W of a thermal electron taking part in the emission process is small compared to W_a, the wave number $\kappa=\hbar^{-1}[2m(W+W_a)]^{\frac{1}{2}}$ is very nearly $\hbar^{-1}[2mW_a]^{\frac{1}{2}}$.

For the potential in region II, the wave equation becomes:

$$d^2\psi/dx^2+2m\hbar^{-2}[W+e^2(4x)^{-1}-\eta e^2(4x^2)^{-1}]\psi=0. \tag{10}$$

Setting $\sigma^2=-2m\hbar^{-2}W$, $\lambda^2=2me^2\hbar^{-2}$, and introducing the change of variable $\rho=2\sigma x$, we now obtain (10) in the form

$$\frac{d^2\psi}{d\rho^2}+\left[-\frac{1}{4}+\frac{\lambda^2}{8\sigma\rho}-\frac{\eta\lambda^2}{4\rho^2}\right]\psi=0.$$

This equation is identically Whittaker's equation,[14]

$$\frac{d^2\psi}{d\rho^2}+\left[-\frac{1}{4}-\frac{k}{\rho}+\frac{\frac{1}{4}-m^2}{\rho^2}\right]\psi=0, \tag{11}$$

with $k=-\lambda^2(8\sigma)^{-1}$ and $m=\pm\frac{1}{2}[1+\eta\lambda^2]^{\frac{1}{2}}$. The solution of (11) is

$$\psi_{\mathrm{II}}=b_1M_{k,+m}+b_2M_{k,-m},$$

where $M_{k,\pm m}$ are the Whittaker confluent hypergeometric functions[14]

$$M_{k,\pm m}=\rho^{\frac{1}{2}\pm m}e^{-\frac{1}{2}\rho}\times\left[1+\sum_{n=0}^{\infty}\frac{\Gamma(1\pm 2m)\Gamma(n+\frac{3}{2}\pm m-k)}{\Gamma(\frac{1}{2}\pm m-k)\Gamma(n+2\pm m)\Gamma(n+1)}\rho^n\right]. \tag{12}$$

To the right of x_2 and extending to a distance of $x(\zeta)$ to the left of the barrier maximum, the WKB approximation is assumed valid. In this region, the general solution is a first-order WKB wave

$$\psi_{\mathrm{III}}=c_1p^{-\frac{1}{2}}\exp\left[i\int_{x_0}p(\xi)d\xi\right]+c_2p^{-\frac{1}{2}}\exp\left[-i\int_{x_0}p(\xi)d\xi\right], \tag{13}$$

with

$$p(x)=\{2m\hbar^{-2}[W+e^2(4x)^{-1}-\eta e^2(4x^2)^{-1}+eFx]\}^{\frac{1}{2}}.$$

In the computation for μ only the transmitted wave, the first term on the right of (13), is used.

The continuity of the wave functions and their derivatives at the join points x_s and x_2 yield four equations for determining the constants μ, b_1, b_2, and c_1:

$$e^{i\kappa x_s}+\mu e^{-i\kappa x_s}=b_1M_1+b_2M_2, \tag{14}$$

$$i\kappa[e^{i\kappa x_s}-\mu e^{-i\kappa x_s}]=b_1M_1'+b_2M_2', \tag{15}$$

$$b_1M_3+b_2M_4=c_1p_2^{-\frac{1}{2}}\exp\left(i\int_{x_0}^{x_2}pd\xi\right), \tag{16}$$

$$b_1M_3'+b_2M_4'=c_1[ip_2^{\frac{1}{2}}-\tfrac{1}{2}p_2^{-\frac{3}{2}}p_2']\times\exp\left(i\int_{x_0}^{x_2}pd\xi\right). \tag{17}$$

To facilitate our work we have introduced the simplifying notation

$$M_1=M_{k,+m} \quad \text{and} \quad M_2=M_{k,-m} \quad \text{at} \quad x_s=(2\sigma)^{-1}\rho_s,$$
$$M_3=M_{k,+m} \quad \text{and} \quad M_4=M_{k,-m} \quad \text{at} \quad x_2=(2\sigma)^{-1}\rho_2,$$

and $p_2=p(x_2)$, hereafter written simply as p. The prime denotes differentiation with respect to the argument of the function, and explicitly the derivatives of the M functions are

$$M'_{k,\pm m}=[-\tfrac{1}{2}+\rho^{-1}(\tfrac{1}{2}\pm m)]M_{k,\pm m}+\rho^{(\frac{3}{2})\pm m}e^{-\frac{1}{2}\rho}\times\sum_{n=0}^{\infty}\frac{\Gamma(1\pm 2m)\Gamma(n+\frac{1}{2}\pm m-k)}{\Gamma(-\frac{1}{2}\pm m-k)\Gamma(n+2\pm 2m)\Gamma(n)}\rho^n. \tag{18}$$

Solving (14)–(17) for μ, we obtain

$$\mu=e^{2i\kappa x_s}\left[\frac{\xi_1f_1+\xi_2f_2+i(\xi_2f_1-\xi_1f_2)}{f_1^2+f_2^2}\right], \tag{19}$$

where

$$f_1=p\kappa[M_2M_3-M_1M_4]-g_1M_1'+g_2M_2', \tag{19a}$$

$$f_2=p[M_1'M_4-M_2'M_3]+\kappa[g_2M_2-g_1M_1], \tag{19b}$$

$$\xi_1=p\kappa[M_2M_3-M_1M_4]+g_1M_1'-g_2M_2',$$

$$\xi_2=p[M_2'M_3-M_1'M_4]+\kappa[g_2M_2-g_1M_1],$$

[14] I. N. Sneddon, *Special Functions of Mathematical Physics and Chemistry* (Interscience Publishers, Inc., New York, 1956), p. 34.

and

$$g_1=(p'/2p)M_4+M_4', \tag{19c}$$

$$g_2=(p'/2p)M_3+M_3'. \tag{19d}$$

Following JI, Sec. II, and JII, Sec. II, we shall employ two complex transmission coefficients in the surface reflection region, where the latter is to be treated as an isolated reflector. The arguments of these coefficients are necessary for computing the phase accumulation of an electron wave making forward and backward transits of this region. Referring to (9) and (13) for notation, we define a forward transmission coefficient

$$T_F=c_1 \quad (c_2=0),$$

and a reverse transmission coefficient

$$T_R=(\mu/c_2).$$

From (14)–(17) we readily obtain

$$T_F=e^{i\kappa x_s}e^{\pi i}\frac{2\kappa p^{\frac{1}{2}}W(M_3;M_4)(f_2+if_1)}{f_1^2+f_2^2}\times\exp\left[-i\int_{x_0}^{x_2}p(\xi)d\xi\right], \tag{20}$$

where f_1 and f_2 are given by (19a) and (19b) respectively and W is the Wronskian,

$$W(M_3;M_4)=M_3M_4'-M_4M_3'. \tag{21}$$

Upon using the appropriate wave functions in regions I and III and proceeding in similar fashion as for μ and T_F, the reverse transmission coefficient is found to be

$$T_R=e^{i\kappa x_s}\frac{2W[-Y_2+iY_1]}{Y_1^2+Y_2^2}\exp\left[-i\int_{x_0}^{x_2}p(\xi)d\xi\right],$$

where

$$Y_1=-\kappa p^{\frac{1}{2}}y_3+\tfrac{1}{2}p^{-\frac{3}{2}}p'y_2+p^{-\frac{1}{2}}y_2,$$
$$Y_2=\tfrac{1}{2}\kappa p^{-\frac{3}{2}}p'y_3-\kappa p^{-\frac{1}{2}}y_4+p^{\frac{1}{2}}y_1,$$
$$W=W(M_1;M_2),$$
$$y_1=M_3M_2'-M_1'M_4,$$
$$y_2=M_1'M_4'-M_2'M_3',$$
$$y_3=M_1M_4-M_2M_3,$$
$$y_4=M_2M_3'-M_1M_4'.$$

B. Numerical Evaluation of μ

The rapid convergence of the series solutions in (12) and (18) makes the numerical computation of μ from the Whittaker functions feasible. As a general check, a lengthier Runge-Kutta numerical integration of (11) was performed to obtain two solutions, say ψ_1 and ψ_2 and their first derivatives. Then since the M's are linear combinations of the ψ functions, we have the following set of equations to determine the M's at x_2 if their boundary values are known at x_s:

$$M(x)=a_1\psi_1+b_2\psi_2, \tag{22}$$

$$M'(x)=a_1\psi_1'+b_2\psi_2'. \tag{23}$$

For a given value of η and W_a, the series solutions for the M's differed by $\sim 1\%$ from those calculated by (22) and (23). The "internal" consistency of the solutions obtained by both methods was checked by noting that the Wronskian for any two independent solutions of (11) is a constant.

IV. CALCULATION OF λ AND δ

The discussion in this section will follow the notation and formalism of Sec. II, JII. In Sec. IV and all subsequent analysis, we shall use atomic units, i.e., distances are in units of the first Bohr radius [$a_0=(me^2)^{-1}\hbar^2=0.529$ A] and energy in units of the hydrogen ionization potential [$W_H=(2\hbar^2)^{-1}me^4=13.58$ ev].

It has previously been shown[2] that the transmission coefficient for the total potential barrier may be written in the following form:

$$D=1-R=1-|(\lambda+\mu)(1+\lambda\mu^*)^{-1}|^2\simeq D_0+D_1+D_2, \tag{24a}$$

where

$$D_0=1-|\lambda|^2, \tag{24b}$$

$$D_1=-|\mu|^2[(1-|\lambda|^2)^2-2|\lambda|^2(1-|\lambda|^2)\cos 2\sigma], \tag{24c}$$

$$D_2=2|\mu||\lambda|(1-|\lambda|^2)\cos\sigma, \tag{24d}$$

$$\sigma=\arg\lambda-\arg\mu+\pi, \tag{24e}$$

$$\lambda=\lambda_0 e^{i(\arg T_F+\arg T_R)}. \tag{25}$$

λ_0 is defined, as in JII, as the reflection coefficient to be attributed to the region B_M considered as an isolated reflector. The expansion on D is made with the assumption that $|\mu|^3\ll 1$.

To calculate λ_0 the following model for the potential is assumed: In region III, where $V(x)$ is given by (8), the WKB approximation, Eq. (13), is used. In the neighborhood of the barrier maximum, the parabolic approximation to the potential is assumed valid:

$$V\cong V_p(x)=-x_0^{-1}-(2x_0^3)^{-1}(x-x_0)^2,$$
$$x(\zeta)\leqslant x\leqslant x(-\zeta).$$

The corresponding wave function, ψ_p, is given in JII.

The formal calculation for λ_0 has been done elsewhere[4,5] so only the final result is given here:

$$\lambda_0=(c_2/c_1)=(1+e^{2\pi\beta\epsilon})^{-\frac{1}{2}}\times\exp\left[i[C+\ln(\zeta^2)]\beta\epsilon+\tfrac{1}{2}\zeta^2+2\int_{x_0}^{x(\zeta)}\kappa_B dx-\tfrac{1}{2}\pi\right], \tag{26}$$

where now, however,

$$\kappa_B=[\epsilon+(x_0-x)^2(2x\,x_0^2)^{-1}-\eta(x)^{-1}(x_0-x)^2(2x\,x_0^2)^{-1}+\eta(x_0-x)(3x_0^2)^{-1}]^{\frac{1}{2}}. \tag{27}$$

The expression for σ given in Eq. (7a) of JII remains unchanged except that κ_B is given by (27).

To evaluate the integral term in (26), we proceed, as in JII, by first expanding κ_B about $\epsilon=0$. To terms of first-order in ϵ Eq. (26) becomes

$$\kappa_B \cong \kappa_0 + \epsilon(2\kappa_0)^{-1} + \tfrac{1}{2}\kappa_0\rho - \epsilon\rho(4\kappa_0)^{-1}, \tag{28}$$

where

$$\rho = -\eta(x)^{-1} + 2\eta x\, x_0^{-1}(x_0-x)^{-1},$$
$$\kappa_0 = \kappa_0(x) = \kappa_B(\epsilon=0).$$

Then, using the approximations (28) and $x_2 \ll x_0$,

$$2\int_{x_2}^{x(\zeta)} \kappa_B dx \cong y - (8x_2)^{\frac{1}{2}} - \tfrac{1}{2}\zeta^2 - [4+\ln(\zeta^2)-\ln y-\ln 12]\beta\epsilon - 4\eta(8x_2)^{-\frac{1}{2}} + \eta[4+\ln(\zeta^2)-\ln y-\ln 12]\beta\epsilon + \tfrac{4}{3}\eta\beta\epsilon. \tag{29}$$

In obtaining (29), the quantity $x(\zeta)^{\frac{1}{2}}$, defined in Eq. (5b) of JII, has been approximated by

$$x(\zeta)^{\frac{1}{2}} \cong x_0^{\frac{1}{2}}[1-(2x_0)^{-1}2\beta^{\frac{1}{2}} - (8x_0^2)^{-1}\zeta^2\beta].$$

Substituting (28) in Eq. (7a) of JII, and letting $\alpha = |\beta\epsilon|$, one obtains

$$\sigma = \sigma_0' \pm g'\alpha, \tag{30a}$$

where

$$\sigma_0' = (y+\pi/2) - \delta', \tag{30b}$$

$$\delta' = \Delta + (8x_2)^{\frac{1}{2}} + (\phi-\phi') + 4\eta(8x_2)^{-\frac{1}{2}}, \tag{30c}$$

$$g' = C - (1-\eta)(4-\ln y-\ln 12) + \eta[\ln(\zeta^2)+\tfrac{4}{3}]. \tag{30d}$$

The quantities ϕ and Δ are still conveniently found from Eqs. (3a) and (3b) of JII. However, ϕ' is now determined by the relation

$$\arg T_F + \arg T_R = \pi + \phi' - 2\Delta - 2\int_{x_0}^{x_2} \kappa_B dx. \tag{31}$$

V. ENERGY AVERAGING OF THE TRANSMISSION COEFFICIENT

The discussion in this section will be restricted to the thermionic Schottky deviations. The transmission coefficient given in Eq. (24) can be expressed as a function of the field and energy by substituting the values of λ_0 and μ from Eqs. (26), (19), Eqs. (3) and (4) of JII, and (30) into (24). The average transmission coefficient $\langle D(F)\rangle_{Av}$ is then found by summing $D(F,W)$ over a Maxwellian distribution of energies. The average of each term, D_n, in Eqs. (24a)–(24d) is defined, in analogy with Eq. (20) of JII, as

$$\langle D_n\rangle_{Av} = \left(\int_0^\infty D_{n+}(\alpha)N_+(\alpha)d\alpha + \int_0^\infty D_{n-}(\alpha)N_-(\alpha)d\alpha\right) \Big/ \int_0^\infty N_+(\alpha)d\alpha.$$

The (+) and (−) signs correspond to the quantities evaluated for the energy range $\epsilon>0$ and $\epsilon<0$, respectively.

After expanding $|\lambda|$ as in JI, D_0, $D_{1\pm}(m)$, $D_{1\pm}(p)$ and $D_{2\pm}$, defined in JI, are more conveniently expressed by (18a), (18b), (18c), and (18d) of JII, except that σ_0' and g' are given by Eq. (30). The functions $N_\pm$ are the Boltzmann factors

$$N_\pm(\alpha) = e^{\mp 2\pi B\alpha}, \tag{32}$$

where $B=(2\pi\beta kT)^{-1}$.

The result of computing the average of D_0 is given in Eq. (10a) of JI. Assuming the high-temperature approximation discussed in JI and discarding all terms in (10a) smaller than $|\mu|B$ or B^2, one obtains

$$\langle D_0\rangle_{Av} = 1 + (\pi B)^2/6, \tag{33}$$

which differs slightly from Eq. (17b) of JI. The average of the periodic term D_1 is the same as Eq. (17c) of JI. In averaging the important periodic term, D_2, certain approximations were used by the authors of JI and JII. We have carried out the averaging process for D_2 without introducing similar approximations and have obtained somewhat different results. Upon inserting (32) into (31), replacing the denominator by $(2\pi B)^{-1}$, and setting

$$D_{2+} = 2|\mu| \sum_{n=0}^{\infty} (-1)^n \frac{\Gamma(n+\frac{3}{2})}{\Gamma(\frac{3}{2})\Gamma(n+1)} \cos(\sigma_0'+g'\alpha)e^{-a_n\alpha},$$

$$D_{2-} = 2|\mu| \sum_{n=0}^{\infty} (-1)^n \frac{\Gamma(n+\frac{3}{2})}{\Gamma(\frac{3}{2})\Gamma(n+1)} \cos(\sigma_0'-g'\alpha)e^{-b_n\alpha},$$

the expression for $\langle D_2\rangle_{Av}$ becomes

$$\langle D_2\rangle_{Av} = 4\pi B|\mu| \sum_{n=0}^{\infty} (-1)^n \frac{\Gamma(n+\frac{3}{2})}{\Gamma(n+1)\Gamma(\frac{3}{2})}[I_n+K_n], \tag{34}$$

where

$$I_n = \int_0^\infty e^{-a_n\alpha}\cos(\sigma_0'+g'\alpha)d\alpha \quad \text{for} \quad \epsilon>0, \tag{35}$$

$$K_n = \int_0^\infty e^{-b_n\alpha}\cos(\sigma_0'-g'\alpha)d\alpha \quad \text{for} \quad \epsilon<0, \tag{36}$$

$$a_n = 2\pi(n+\tfrac{1}{2}+B) \quad \text{for} \quad \epsilon>0, \tag{37}$$

$$b_n = 2\pi(n+1-B) \quad \text{for} \quad \epsilon<0. \tag{38}$$

When the integrals are evaluated, (34) becomes

$$\langle D_2\rangle_{Av} = 4\pi|\mu|B \sum_{n=0}^{\infty} (-1)^n \frac{\Gamma(n+\frac{3}{2})}{\Gamma(n+1)\Gamma(\frac{3}{2})} \times\{[a_n^{-1}(1+G_n^2)^{-1} + b_n^{-1}(1+J_n^2)^{-1}]\cos\sigma_0' + [G_n a_n^{-1}(1+G_n^2)^{-1} - J_n b_n^{-1}(1+J_n^2)^{-1}\sin\sigma_0']\}. \tag{39}$$

In (34), G_n and J_n are defined by

$$G_n \equiv g'/a_n, \quad J_n \equiv g'/b_n.$$

Since the factor g' is a function of the applied field, the summation in (39) must be performed for different values of g' and a relation developed for $\langle D_2\rangle_{Av}$ of the form

$$\langle D_2\rangle_{Av}=4\pi|\mu|Bf_3(y)\cos[\sigma_0'+f_4(y)]. \quad (40)$$

From (30d) it is seen that g' varies slowly with ζ. Therefore it is adequate to choose a mean value of ζ for all computations. For a characteristic field, say $F\cong 10^5$ volt cm^{-1}, the parabolic approximation to the potential V_p, was compared to the true potential $V(x)$. The choice of ζ was determined by finding where V_p differed from $V(x)$ by 1%.

If the limiting values of field are 10^3 volt cm^{-1} to 2×10^6 volt cm^{-1}, then g' lies between 4.47 and 2.82. Numerical computations for determining $f_3(y)$ and $f_4(y)$ were made for four g' values. To facilitate the evaluation of (39), the summation was broken up into three ranges within which appropriate approximations were applied:

$$\sum_{n=0}^{\infty}=\sum_{n=0}^{N'}+\sum_{n=N'+1}^{N''}+\sum_{n=N''+1}^{\infty}, \quad (41)$$

where for the computations N' and N'' were taken to be 25 and 45, respectively. For the first N' terms, the only approximation is to neglect B in a_n and b_n when the index $n\geq 5$. Since $B\leq 0.1$ for $T\geq 1000$°K and $F\cong 10^5$ volt cm^{-1}, this results in an error of less than 1% in each term of the first sum.

In the range of n covered by the second sum on the right of (41), both G_n and J_n are much less than unity. Therefore this sum contributes a value independent of g':

$$\sum_{n=N'+1}^{N''}=\sum_{n=N'+1}^{N''}(-1)^n\frac{\Gamma(n+\frac{3}{2})}{\Gamma(n+1)\Gamma(\frac{3}{2})}[a_n^{-1}+b_n^{-1}]\cos\sigma_0'.$$

The coefficient of $\sin\sigma_0'$ can be neglected with an error of less than 1%.

In the last sum on the right side of (41) the values of n are such that $a_n\cong b_n$ and the Sterling approximation to the gamma function,

$$\Gamma(n)\cong(2\pi)^{\frac{1}{2}}e^{-n}n^{n-\frac{1}{2}},$$

is valid. This sum then becomes

$$2\pi^{-\frac{3}{2}}e^{-\frac{1}{2}}\sum_{n=N''+1}^{\infty}(-1)^n n^{-\frac{1}{2}}. \quad (42)$$

The summation in (42) can be rewritten as

$$\sum_{j=0}^{\infty}\{[n+2j]^{-\frac{1}{2}}-[n+2j+1]^{-\frac{1}{2}}\}, \quad (43)$$

where n is now equal to $N''+1$. If n is taken large enough, then the term in curly brackets can be considered as equal to

$$-\frac{d}{dj}\{2^{-1}[n+2j]^{-\frac{1}{2}}\}=2^{-1}[n+2j]^{-\frac{3}{2}}. \quad (44)$$

Inserting (44) into (43) and assuming a continuous distribution on j, one obtains

$$\sum_{n=N''+1}^{\infty}\rightarrow\tfrac{1}{2}\int_0^{\infty}(n+2j)^{-\frac{3}{2}}dj.$$

The contribution of the final term of (41) is, therefore,

$$\sum_{n=N''+1}^{\infty}\cong\pi^{-\frac{3}{2}}e^{-\frac{1}{2}}(N''+1)^{-\frac{1}{2}}. \quad (45)$$

When the summations are carried out it is found that the functions $f_3(y)$ and $f_4(y)$ can be represented by the equations

$$f_3(y)\cong 4.4y^{-0.3}, \quad (46a)$$

$$f_4(y)\cong 0.226y^{0.14}. \quad (46b)$$

Since $f_4(y)$ varies by less than 0.1 of a radian over the entire range of F, it can be replaced by its average value. Upon using (46a) and $\langle f_4(y)\rangle_{Av}$, the final average for D_2 is

$$\langle D_2\rangle_{Av}\cong 17.6\pi y^{-0.3}|\mu|B\cos(\sigma_0'+0.4). \quad (47)$$

If we let $\langle D(0)\rangle_{Av}=1-|\mu|^2$ be the zero-field transmission coefficient, then the averaged total transmission coefficient can be written as

$$\langle D\rangle_{Av}=\langle D(0)\rangle_{Av}+\langle D(B)\rangle_{Av}, \quad (48)$$

where

$$\langle D(B)\rangle_{Av}=\tfrac{1}{6}(\pi B)^2+17.6\pi y^{-0.3}|\mu|B\cos(\sigma_0'+0.4). \quad (49)$$

VI. THERMIONIC SCHOTTKY DEVIATIONS

To calculate the monotonic and periodic deviation terms, F_1 and F_2, we substitute (48) into the current density formula for Schottky emission:

$$j=A\langle D(F)\rangle T^2\exp[-(\varphi-F^{\frac{1}{2}})(kT)^{-1}],$$

where φ is the thermionic work function for $F=0$, and $A=4\pi mk^2eh^{-3}$. Then, letting j_0 be the zero-field current density and taking the logarithm of j/j_0, we obtain

$$\begin{aligned}\ln(j/j_0)-mF^{\frac{1}{2}}&=\ln[\langle D(F)\rangle_{Av}/\langle D(0)\rangle_{Av}]\\&\cong\ln\{[1-|\mu|^2+\tfrac{1}{6}(\pi B)^2+\langle D_2\rangle_{Av}][1-|\mu|^2]^{-1}\}\\&=F_1+F_2, \quad (50)\end{aligned}$$

where $m=$ the Schottky slope $=(kT)^{-1}$ and the terms on the right side of (50) constitute the deviations from the simple Schottky theory. By expanding the denominator in (50), retaining only second-order terms and making the approximation $\ln(1+x)\cong x$ in the resulting expression, Eq. (50) becomes

$$\ln(j/j_0)-mF^{\frac{1}{2}}\cong\tfrac{1}{6}(\pi B)^2+\langle D_2\rangle_{Av}=F_1+F_2. \quad (51)$$

Then, substituting (47) and (30b) into (51), inserting numerical values for B, and changing to the common logarithm, we obtain the final expressions for the deviation terms for the thermionic Schottky effect:

$$F_1 \cong 4.0\times 10^{10} T^{-2} y^{-6}, \tag{52}$$

$$F_2 \cong 4.6\times 10^{5} y^{-3.3} T^{-1} |\mu| \cos(y+\tfrac{1}{2}\pi-\delta'+0.4). \tag{53}$$

The small nonperiodic term F_1 is identical in its dependence on field and temperature with the expressions obtained by Juenker[4] and Miller and Good[5] and differs only in a numerical factor from their results. Since the monotonic deviations have not been conclusively observed, the theory is compared with the experimentally observed periodic term F_2. For purposes of comparison the periodic term F_2 found in the previous theories are given here:

$$(F_2)_J = 4.9\times 10^{5} |\mu| T^{-1} y^{-3.3} \cos(y+\tfrac{1}{2}\pi-\delta+0.6), \tag{54}$$

$$(F_2)_{MG} = 4.6\times 10^{5} |\mu| T^{-1} y^{-3.2} \times \cos(y+\tfrac{1}{2}\pi+\arg\mu+\theta), \tag{55}$$

where θ is a phase factor which varies very slowly with the applied field. If the model for calculating μ is left unspecified, then (53), (54), and (55) are almost identical in form.

The theoretically predicted field-dependent factors in the amplitude and period of the periodic deviations have very good experimental confirmation. But the amplitude and phase are also functions of μ, and when the model for the surface potential barrier is specified as the conventional image force with discontinuous slope, the predicted phase of the deviations differ from the observed phase by about $\pi/4$. Moreover, there is lack of agreement between theory and experiment in the amplitude of the periodic deviations. This is illustrated in Fig. 3(a) where (54) and (55), with $T=1500°$K, $W_a=10$ ev, and μ determined by this model, are compared with the available experimental data for the refractory metals. (The results of the two expressions are practically indistinguishable and are plotted as a single curve.) By way of comparison, in Fig. 3(b), the present theory based on the potential of Fig. 2 and with the parameter η equal to $(\frac{3}{16})x_1$, is compared with the same experimental curves.

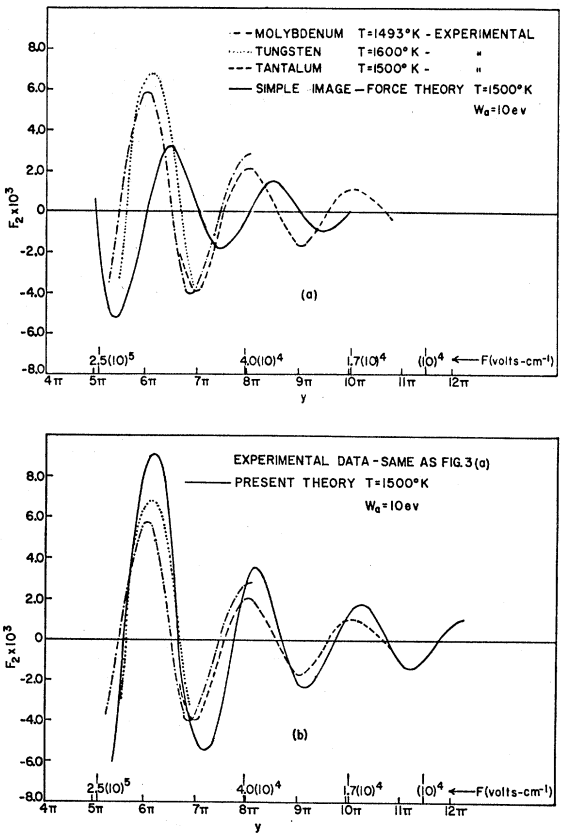

FIG. 3. Comparison of the experimental and theoretical Schottky deviations F_2 as a function of $y=357.1\ F^{-\frac{1}{2}}$ (F in volt cm^{-1}). The solid lines represent the theoretical curves for $T=1500°$K and $W_a=10$ ev: in Fig. 3(a) according to the simple image-force model employed in JI, JII and by Miller and Good; in Fig. 3(b) for the model used in the present theory. Smooth curves have been drawn through the experimental points. For tungsten, the experimental data exhibited a bad patch break in the $F^{\frac{1}{2}}\cong 100$–300 region and only the half-cycle curve in Fig. 3 could be used with assurance. References: tungsten, A. L. Houde, Ph.D. dissertation, University of Notre Dame, 1952 (unpublished); tantalum, reference 3, Fig. 3; molybdenum, G. A. Haas and E. A. Goomes, Phys. Rev. **100**, 640 (1955).

VII. DISCUSSION AND CONCLUSIONS

It has already been noted that the terms $|\mu|$ and δ are determined by the form of the potential at the surface of the metal. Since these parameters can be empirically determined from the amplitude and the location of the maxima and minima of the experimentally measured deviations, comparison can be made with the values of these terms predicted from theory. In Table I we have summarized the measured values of the parameters, those calculated for the simple image-force model, and those given by the present theory.

The data for $|\mu|_{\text{exp}}$ and $\langle\delta_{\text{exp}}\rangle$ are quite similar for all three metals and, as may be noted from Fig. 3, within experimental error the deviations for the three are almost indistinguishable. This is not surprising when one considers that tungsten, tantalum, and molybdenum are all b.c.c. lattices with similar surface structure on corresponding crystal faces and hence have about the same electron-emission properties. It is then questionable whether, in the framework of existing theory, the apparent experimental differences between the three are significant enough to be considered at present. Moreover, when these parameters are computed for the box model (see lines 3 and 5, Table I), the values obtained using the three different W_a's are practically equal and a single mean value of each of the parameters could equally well be used for all three emitters (see last column, Table I). This is also true

TABLE I. Summary of the values of the surface parameter $|\mu|$ and the phase factor δ as determined from the experimental Schottky deviations and computed for the different surface potentials. The experimental values are taken from Table I of JI and Table I of JII. The single dagger denotes the theoretical calculations for the box model [JI, JII], and the double dagger the values of $|\mu|$ and δ' computed from Eqs. (19) and (30a) of the present theory. Most probable value of δ_{exp} for molybdenum is indicated by an asterisk.

	Tungsten	Tantalum	Molybdenum	Mean value
W_a	10.3 ev	9.3 ev	10.2 ev	
$\|\mu\|_{exp}$	0.39–0.46	0.39–0.45	0.30–0.42	$\simeq$0.4
$\|\mu\|_{cal}$†	0.22	0.21	0.22	0.22
$\langle\delta_{exp}\rangle$	2.1 –2.3	1.9 –2.2	2.8 –2.3*	$\simeq$2.2
δ_{cal}†	3.6	3.8	3.7	3.7
$\|\mu\|_{cal}$††	0.61	0.61	0.61	0.6
δ_{cal}'††	2.6	2.6	2.6	2.6

for the present theory where one value of $|\mu|_{cal}$ and δ'_{cal} calculated for $W_a=10$ ev, suffices for all three metals. We shall correspondingly take a single mean experimental value for $|\mu|$ and for δ with which to compare the theoretical results.

The surface potential proposed in the present theory yields good agreement in the observed and predicted phase term δ. There is also improved agreement between theory and experiment in the surface parameter $|\mu|$. The seemingly high values of $|\mu|_{exp}$ found from the periodic deviations have always been regarded with suspicion because they disagreed with the predictions of the Nordheim[15]-MacColl[16] and Miller-Good[5] calculations of the reflection coefficients for a one-dimensional image-force potential. Juenker[4] has suggested that local effects, such as patches, surface irregularities, and contaminations, would produce low rather than high apparent values of $|\mu|_{exp}$. On the other hand, some recent experimental results on the elastic reflection of slow electrons from carefully cleaned metals are in marked disagreement with the previously mentioned theories. In particular, for electron energies of the order of the work function of the metals, the values of $|\mu|^2$ for tungsten[17] and molybdenum[18] were found to be $\lesssim$0.25 and 0.18, respectively—values consistent with results from the periodic deviations.

Thus the analysis, even if restricted to a one-dimensional potential approximation, can yield satisfactory agreement with experiment when the simple image-force law is modified in a manner suggested by quantum mechanical considerations. Certain improvements in the procedure might suggest themselves, such as smoothing the derivative of the potential at the join with W_a and correcting for the approximation $|\mu|^3 \ll 1$.[19] Moreover, it is realized that the shape of our potential minimum, selected for mathematical convenience, should probably be somewhat broader and shallower. However, in the present state of the theory such second-order corrections seem to be unwarranted.

ACKNOWLEDGMENTS

The authors wish to express their gratitude to Professor E. A. Coomes and Professor D. W. Juenker of the University of Notre Dame for making available certain experimental data and for their valuable comments and criticism of the manuscript. We also wish to express our appreciation for helpful discussions with Professor R. H. Good of Iowa State College and Dr. C. Herring of the Bell Telephone Laboratories.

One of us (P. H. C.) gratefully acknowledges the award of a fellowship from the Haloid Company, Rochester, New York, during 1956–1958.

[15] L. Nordheim, Proc. Roy. Soc. (London) **A121**, 626 (1928).
[16] L. A. MacColl, Phys. Rev. **56**, 699 (1939).
[17] D. A. Gorodetski, Bull. Acad. Sci. U.S.S.R.—Physical Sciences **20**, 1023 (1955). (For English translation see Columbia Technical Translations.)
[18] A. R. Shulman and E. I. Miakinin, J. Tech. Phys. **26**, 2223 (1956) [translation: Soviet Phys., Tech. Phys. **1**, 2157 (1957)].
[19] See, for example, the discussion in reference 4, Sec. V.